Microfluidic investigation of crude oil droplet coalescence: effect of oil/water composition and droplet ageing

Marcin Dudek[1,†], Julien Chicault[2] and Gisle Øye[1]

[1] Ugelstad Laboratory, Department of Chemical Engineering, Norwegian University of Science and Technology (NTNU), Trondheim, Norway

[2] National Graduate School of Engineering (ENSICAEN), Caen, France

† Corresponding author: marcin.dudek@ntnu.no ; Sem Sælandsvei 4, 7491 Trondheim, Norway

ABSTRACT

The coalescence between crude oil droplets is a major factor influencing the efficiency of most produced water treatment processes. As the droplets grow bigger in size, it is easier to remove them from the continuous water phase, which will improve the quality of produced water and help meet increasingly stricter environmental and process regulations. Here we investigate the coalescence process of crude oil drops in water with the use of previously reported microfluidic tools. It was shown that the composition of both oil and water phases heavily impacts the merging between droplets, both outcome (final droplet size distribution) and the kinetics of the phenomena (coalescence time). In the droplet ageing experiments, the coalescence was always most extensive for the droplets with the shortest ageing time, while the coalescence typically decreased with increasing droplet size distribution, however this

was oil-specific. Overall, the results underline the importance of crude oil and produced water chemistries during the water treatment process.

1. INTRODUCTION

Treatment of produced water (PW) is becoming the dominating separation process during production of crude oil and natural gas. While at the Norwegian Continental Shelf (NCS) the water-to-oil ratio is approximately 2:1, globally this ratio is closer to 4:1, and it will keep increasing in the future. PW has a complex composition, consisting of both dispersed and dissolved components of organic and inorganic nature. In an offshore facility, the water is typically discharged after treatment, however more operators decide to re-inject the produced water either for pressure support or discharge.

Most produced water treatment processes focus on the dispersed droplets and particles, as these cause serious environmental and process concerns. The majority of regulations limit the discharge of dispersed crude oil to 30-40 ppm, whereas re-injection criteria can be as strict as 5 ppm of dispersed particles below certain size [1]. For this reason, water separation processes must be efficient and able to remove even very small droplets from the water phase. The performance of many of them relies on the oil droplet size. In separators like skimmers or hydrocyclones, the separation is based on Stokes law, which relates the physical properties of the fluids (density, viscosity), and the droplet size to its rising velocity. The square dependency of the droplet diameter implies that this parameter is the dominating factor in the process [2]. Moreover, in gas flotation, the efficiency of the separation is dictated by the bubble-droplet interactions, which are greatly influenced by their relative sizes [3, 4]. Also in membrane separation, the droplet size is an important factor [5].

The main process controlling the droplet growth is coalescence. It is often described with three distinct stages [6]: (1) droplet collision and formation of a thin film between drops; (2)

film drainage; (3) film rupture and merging of two drops (Figure 1). Collisions are typically the result of hydrodynamics in the system, e.g. turbulence, buoyancy or Brownian motion. The film drainage, however, is a more complex process and can be a function of hydrodynamics, fluid properties and colloidal forces. If the time necessary to drain the film is longer than the average contact time between drops, the droplets will often detach and flow apart. The film drainage is the controlling factor in the kinetics of coalescence, however in static conditions the duration of the film rupture and merging might also be significant [7].

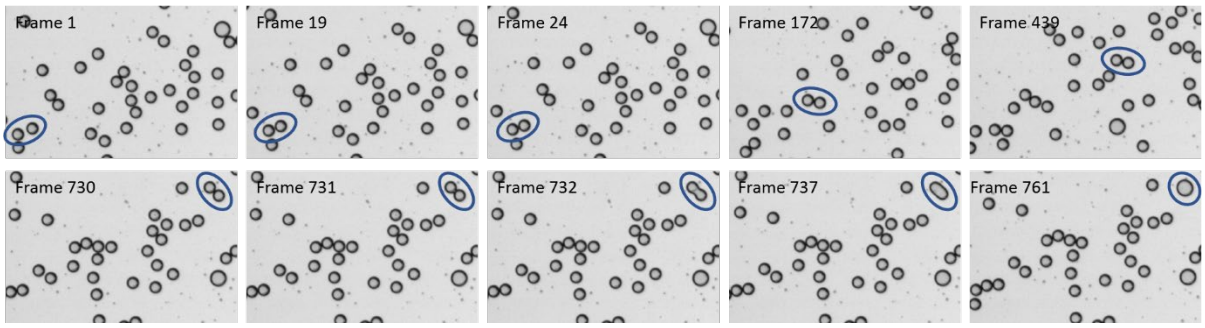

Figure 1 Consecutive frames showing different stages of coalescence: approach (frames 1 to 24), collision (frame 24), film drainage (frames 24-730), film rupture (frame 732) and droplet fusion (frames 732-737). The time between two frames is approx. 75 µs, therefore coalescence time is equal to 52.1 ms.

Crude oil is a complex mixture of hydrocarbons. It contains a variety of species that are considered surface-active, such as resins, asphaltenes and naphthenic acids. These can affect the coalescence between drops in different ways [7]. In a similar fashion, the water composition and properties will be important for the emulsion stability [8, 9]. The coalescence between oil droplets will also depend on the hydrodynamic conditions, like fluid velocity or turbulence level. Disturbances in the flow can lead to collisions between droplets, however too high turbulence can cause drop breakage [10]. In addition, when a crude oil drop is created out of the continuous phase, the surface-active components start to diffuse to the freshly made oil-water interface. This interfacial ageing of the droplet affects the coalescence process through, for example, building up elastic interfacial layers and decreasing the interfacial tension value [11].

Treatment of emulsions closer to wellheads (where the emulsions often are generated), e.g. through subsea treatment of fluids, can therefore prove beneficial for separation.

In petroleum research, most of the emulsion stability and coalescence studies are performed on oil-continuous systems [12-20], whereas less data is available for produced water systems. Peru and Lorenz used a setup based on a spinning drop method to measure the coalescence time of two crude oil droplets in alkali solutions [21]. The setup of Ata et al. allowed to generate two equal-sized drops through capillaries and follow their coalescence [22], however they focused on studying the merging of petroleum-derivatives rather than real crude oils. Gaweł et al. measured the drainage and rupture times between two crude oil drops using a modified pendant drop technique (DBMM – droplet bubble micro manipulator) [7]. They showed that coalescence was reduced by elasticity of the interface caused by poor solubility of asphaltenes in the crude oils. Another setup, with improved control over the approach velocity of the two droplets was utilized Ayirala et al., who measured the coalescence times of crude oil drops in the presence of different inorganic ions [23, 24]. The coalescence in produced water systems was also studied in dynamic systems. Sterling et al. investigated the kinetics of coalescence of crude oil droplets in a batch reactor [25]. A stirring tank was used by Angle et al., who followed the change in size distributions of toluene-diluted heavy oil in water emulsions upon variation of different parameters [10, 26, 27]. Some studies also attempted to correlate the crude oil composition with the water quality after separation. Silset et al. conducted bench and technical scale experiments with a large matrix of oils to map the relation between the crude oil properties and the separation performance [28]. Eftekhardadkhah and Øye investigated the effect of the crude oil and water composition on the concentration and interfacial activity of the dissolved components in produced water [29]. Their study showed good correlation between the water quality and the presence of certain heteroatom-containing groups in crude oils. The present authors also published a paper on the effect of oil and water

compositions on the separation of crude oil emulsions and water quality after gravity separation [9].

Recently, microfluidics has been used to study the emulsion stability and behaviour [30]. This technique offers the advantage of performing systematic measurements in relatively short time. In addition, the drop size range is relevant for the process application, as the oil droplets removed during various water treatments will typically be tens of μm in diameter. In the petroleum research, both oil-in-water [31] and water-in-oil [32-34] systems were reported.

Previously we have reported the results of coalescence in microfluidic channels of three crude oils in various water phases [31]. In this paper we use a similar methodology, but extend the experimental matrix to ten crude oils, more complex water compositions and additionally investigate the effect of droplet ageing. We also show how different water phases can affect the coalescence time of various crude oils.

2. EXPERIMENTALS

2.1. Chemicals.

Crude oils. The physical properties and composition of crude oils are summarized in Table 1.

Table 1 Physicochemical properties of crude oils.

Crude oil	API [°]	Viscosity [mPa s] @20°C	TAN [mg KOH/ g oil]	TBN [mg KOH/ g oil]	SARA [% wt.]			
					Saturates	Aromatics	Resins	Asphaltenes
B	35.8	14.2	<0.1	1.0	84.0	13.4	2.3	0.3
E	37.9	8.3	0.5	0.4	74.8	23.2	1.9	0.1
F	39.7	7.5	<0.1	0.6	78.5	18.9	2.5	0.1
G	34.5	12.4	0.2	0.6	83.4	14.0	2.4	0.2
H	46.9	2.2	<0.1	0.3	84.8	13.7	1.4	0.1
I	38.4	5.8	<0.1	0.4	87.2	11.6	1.1	0.1
J	28.5	17.4	0.6	1.2	74.6	19.7	5.3	0.4
K	35.2	10.4	<0.1	1.0	74.2	20.5	4.5	0.8
P3	31.7	14.7	<0.1	0.7	51.6	40.4	5.8	2.2
P5	45.0	6.9	<0.1	0.2	82.5	16.7	0.7	0.1

In order to reduce the adsorption of crude oil to glass walls of the microfluidic chip, 200 ppm of the same surfactant was added to all crude oils. The densities and viscosities were measured with a DMA 5000M (Anton Paar) and an MCR 301 laboratory rheometer (Anton Paar), respectively, at 20°. Total acid and base numbers (TAN and TBN, respectively) analysis was conducted as described in detail previously [9]. Briefly, TAN was measured by

potentiometric titration of a solution of petroleum in 100:99:1 (v/v) toluene/isopropanol/water mixture with a solution of tetrabutylammonium hydroxide (0.1M). For TBN measurements, the crude oil was dissolved in methylisobutyl ketone and titrated with a solution of perchloric acid in acetic acid (0.025M). The details of SARA (saturates, aromatics, resins and asphaltenes) analysis were reported elsewhere [35]. In short, 160 ml of n-hexane was added to 4 g of crude oil and stirred overnight. The mixtures were then filtered to separate the precipitate (asphaltene fraction), which weight was noted. The filtrate (maltenes) were run through an HPLC system with two columns (unbonded silica and amino) to separate saturates, aromatics and resins. After collecting the fractions, the samples underwent evaporation in nitrogen atmosphere and weighted to determine weight fractions.

Produced water. Several types of brines were used in this study. Pure sodium chloride solution and sodium chloride with the addition of calcium chloride (Ca/Na molar ratio of 1/35) at equal ionic strength were used to study the effect divalent ions on coalescence. The natural pH of the brines ranged between 5.8 and 6.6, and for clarity these are later referred to as pH 6. The pH was adjusted to pH 4 and 10 with diluted solutions of NaOH and HCl. The synthetic produced water (SPW) had a considerably higher salinity (more than 10% of total dissolved solids) and contained Na^+, Ca^{2+}, Mg^{2+} cations and Cl^-, HCO^{3-} and SO_4^{2-} anions (detailed composition reported in Table S1 in SI). The pH of SPW was close to 7. To avoid precipitation of carbonates, the brine was kept in a refrigerator and taken out an hour before the measurements to bring it to room temperature. The preparation of brine with dissolved Fluka naphthenic acids at pH 6 was described in SI. The brine was diluted with sodium chloride brine to contain ca. 100 ppm of acidic species. All aqueous solutions were prepared with deionized water (Millipore Simplicity Systems).

2.2. Microfluidic chips and setup. The microfluidic setup and the designs of the microfluidic chips are illustrated in Figure 2.

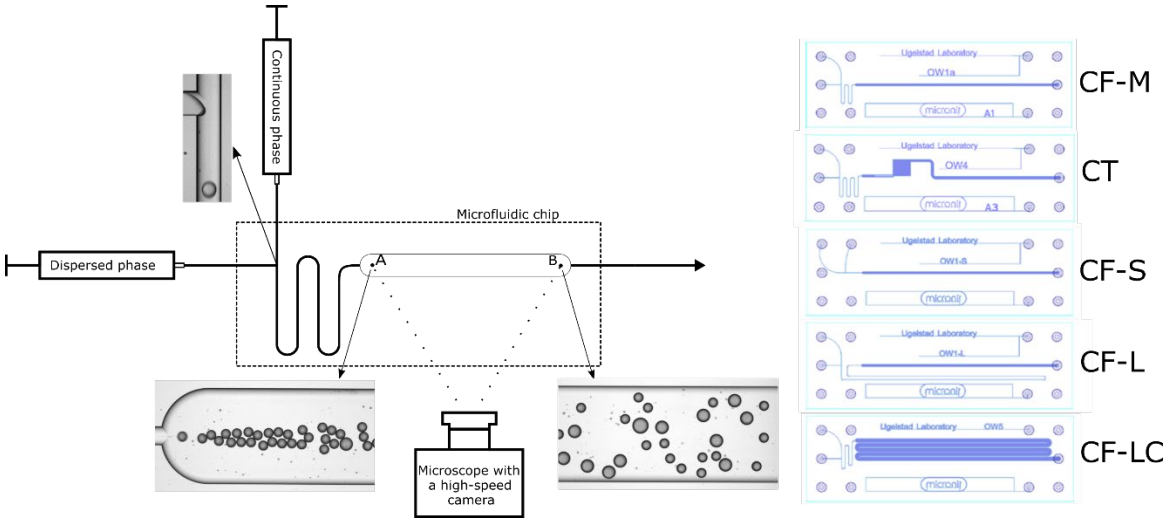

Figure 2 Illustration of the microfluidic setup and chips. CF refers to chips used for studying coalescence frequency with short, medium and long meandering channels (S, M and L, respectively) or with a long coalescence channel (LC). Chip CT was used to determine the coalescence time. Table 2 contains detailed description and use of chips in specific sections.

Glass microfluidic chips were custom-designed and delivered by Micronit Microtechnologies B.V. All had a T-junction, where the two inlet channels (100 µm wide) met and droplets were generated. After passing a meandering channel, the droplet entered a larger chamber, where they could collide and undergo coalescence. The outlet was located on the other end of the chamber. The dimensions of both meandering channels and coalescence chamber were different for all the chips, and are summarized in Table 2. All channels had a uniform depth of 45 µm. The chips were connected to syringe pumps (neMESYS mid-pressure module V3, Cetoni GmbH) via a Fluidic Connect PRO chip holder (Micronit Microtechnologies B.V.) with FFKM ferrules and PEEK tubing. After the experiments, the chips were sonicated for 15 minutes in each of the following solvents: toluene/acetone mixture (3:1 v/v), 1% v/v Decon 90™ solution in water, isopropanol and deionized water. Finally, they were put in an ashing

furnace for six hours at 425°C. In addition, the chips were treated in low-pressure oxygen plasma chamber (Zepto, Diener electronic GmbH) for 10 minutes shortly before the experiments.

Table 2 Summary of microfluidic chip dimensions.

Microfluidic chip design	Meandering channel length [mm]	Coalescence chamber dimensions WxL [mm]	Section, in which chips were used
CF-M	15	0.5x33	Oil/water comp. Droplet ageing
CT	15	3x3	Coalescence time
CF-S	3	0.5x33	Droplet ageing
CF-L	75	0.5x33	Droplet ageing
CF-LC	15	0.75x165	Droplet ageing

2.3. Microfluidic experiment, data acquisition and image analysis.

The experiments were performed in similar fashion as in previous reports [31, 36]. Briefly, the flow of oil and water phases were set to 8-10 and 160 µl/min, respectively. The flow of oil was adjusted to keep the number of generated droplets constant (ca. 1 400-1 500 drops per second), regardless of the oil phase. The coalescence experiments were recorded with a high-speed camera (AX100, Photron), connected to an inverted microscope (Ti-U Eclipse, Nikon) with a LED light source (pE-100, CoolLED) at a constant framerate of 8 500 or 13 600 (coalescence time section) frames per second and shutter speed of 1/50 000.

For all measurements involving designs CF-S, -M and -L, two recordings at the inlet and outlet of the chip were taken for each experiment. In the experiments with CF-LC, a total of six sets of images were taken – first at the inlet and the rest at a 33 mm interval (before each U-turn of the serpentine channel), which allowed to determine the size distribution of droplets as a function of the residence time. Approx. 10 000 frames were taken for each recording. The total residence time in the coalescence chamber for the CF-LC was ca. 3 seconds, compared to ca. 0.4 seconds for the other chips. The details of the chip design, experimental

procedure and data analysis of the coalescence time measurements were reported in another work [37].

The recorded series of images were batch-processed with ImageJ by first converting to binary images and later extracting droplet positions and areas with the built-in Analyse Particle feature. The data was treated with a custom-written Matlab script, which was used to sort detected objects into several size classes. The coalescence frequency, which was the main parameter used to compare the extent of merging in the channel, was calculated by comparing the initial and final droplet numbers, and dividing by the residence time in the channel. In the experiments with the CF-LC chip, the values of coalescence frequencies are calculated based on the droplet distribution and residence time at the specific part of the channel. Therefore, these values show the coalescence frequencies between the inlet to the coalescence chamber and the part where the recording was taken, and do not refer to the change in drop size distribution between specific parts of the coalescence channel. All reported data is an average of at least three parallels with the standard deviation shown as error bars.

Partial Least Squares (PLS) regression was performed to identify the most important factors contributing to coalescence frequency between oil droplets. Here, the data was divided into two sets: coalescence in all pH 4 and 6 brines; and coalescence in all pH 10 brines. The X-variables were the physicochemical properties of the crude oils (Table 1), whereas the Y-variables were the averaged coalescence frequencies in the two above mentioned data sets. Preliminary analysis was performed with all factors, which allowed to identify the variable importance in projection (VIP) scores and re-model the data using X-variables with a score higher than 0.8. The data was processed using JMP Software (SAS Institute).

3. RESULTS AND DISCUSSION

3.1. Oil and water composition effect

The coalescence of crude oils in sodium chloride brine at different pH levels is presented in Figure 3.

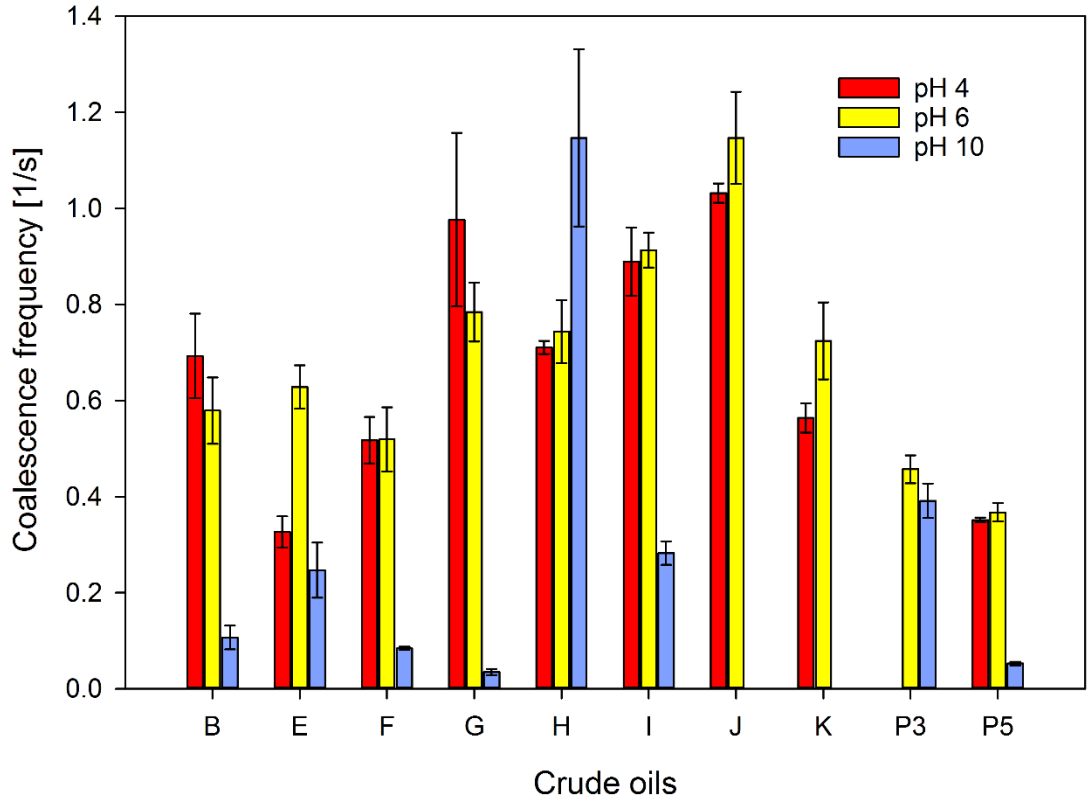

Figure 3 Coalescence frequencies of crude oils in sodium chloride brine at pH 4, 6 and 10.

The coalescence of crude oils depended both on the oil type and the water pH. Typically, most coalescence was observed for the two lowest pH values. Crude oils B and G coalesced more readily in pH 4 than in pH 6, whereas the opposite was true for crude oils E, J and K. The rest of the oils had similar coalescence frequency values in both pH conditions. The measurement for crude oil P3 in brine at pH 4 could not be performed due to excessive wetting of the oil on the walls of the glass chip. In the highest pH, the coalescence was

significantly lowered with two marked exceptions: crude oil P3, where the coalescence did not change compared to pH 6; and crude oil H, where the merging was more extensive. In two cases (J, K), the coalescence analysis was not possible due to the excessive deformation and breakage of droplets in the channel, most likely because of too low interfacial tension values in these conditions (similar phenomenon was observed for the diluted crude oil C in our previous work [31]). Also, no coalescence at pH 10 was observed for both oils.

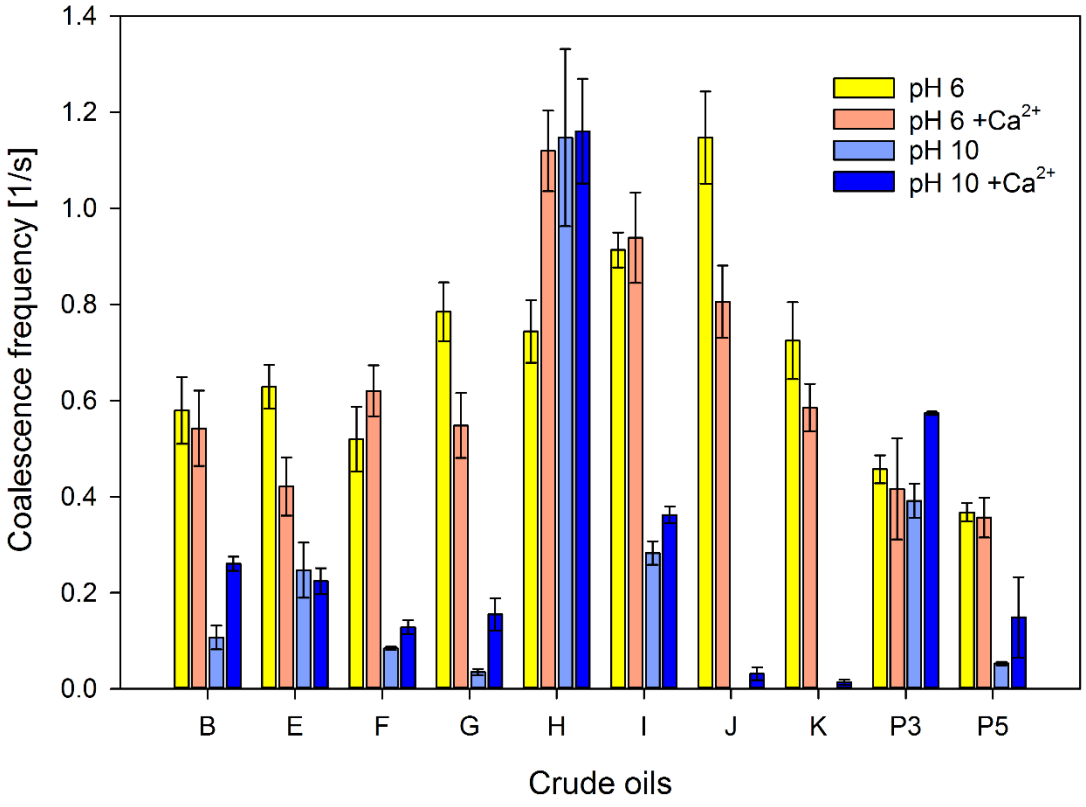

Figure 4 Coalescence frequencies of crude oils in sodium chloride brines with and without calcium at pH 6 and 10.

Figure 4 shows the impact of the addition of calcium ions on the coalescence, compared to the pure sodium chloride brine. At pH 6, only crude oil H had higher coalescence frequency in the brine containing divalent ions. All other oils either coalesced less in the presence of calcium (E, G, J, K) or there was hardly any difference between the two water phases (B, F, I,

P3, P5). At pH 10, however, the effect of calcium was practically the same for all the oils – it led to an increase of merging between drops. Only crude oil E and H had similar values of coalescence, irrespective of the presence of the divalent ions. Interestingly, the addition of calcium to the water phase also allowed to conduct the experiments at high pH with crude oil J and K, which was not possible in pure sodium chloride brine. Still, coalescence was minimal.

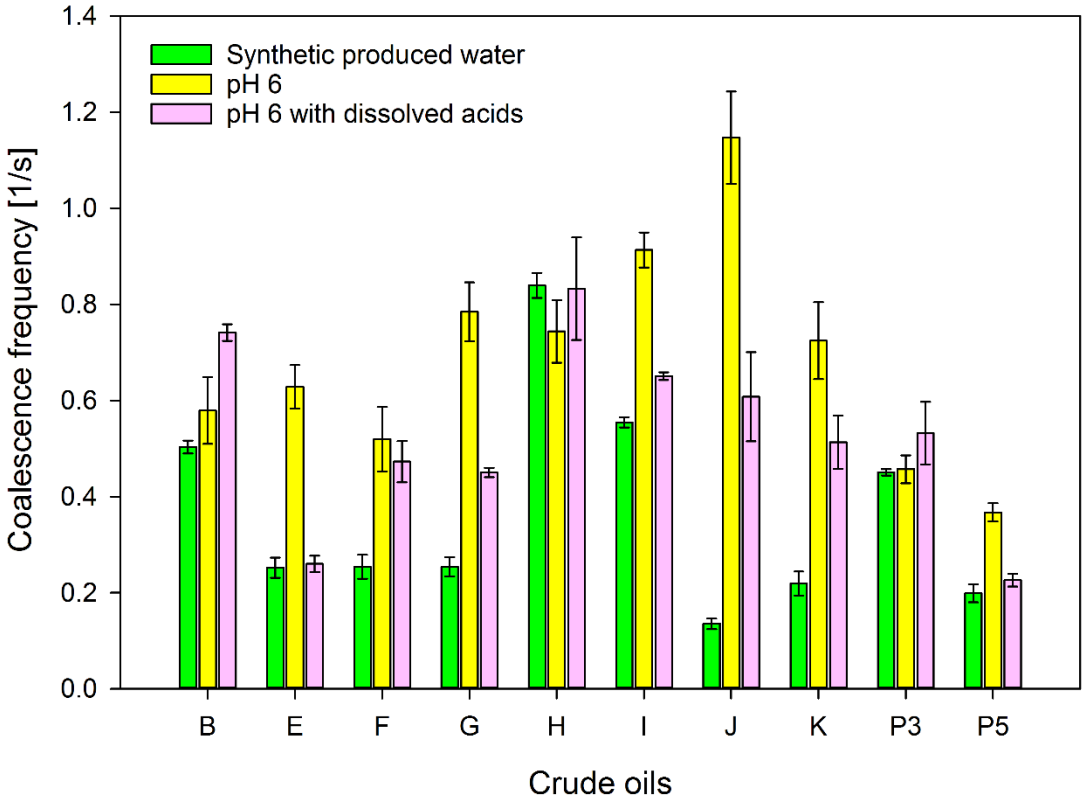

Figure 5 Coalescence frequencies of crude oils in sodium chloride brine at pH 6 with and without dissolved naphthenic acids, and in synthetic produced water.

The effect of more complex ionic composition of brine and the dissolved components is illustrated in Figure 5. The coalescence in synthetic produced water was significantly lower than the merging in simple sodium chloride brine, with an exception of crude oils B, H and P3. The same oils (with the addition of crude oil F) had either higher or the same coalescence

frequency values in the brine containing dissolved acidic components, compared to the standard brine.

The interfacial activity of crude oil components such as resins, asphaltenes and naphthenic acids depends on many factors, like water pH, salinity and ionic composition of the brine. The type of components at the oil-water interface will also determine its properties, e.g. the strength and elasticity of the interfacial layers. All of these factors can influence coalescence of crude oil droplets, as is evident from Figures 3 to 5. At lower pH, the basic components of crude oil will become protonated and probably dominate the interface. They are, however, considered less interfacially-active than acidic components [38-40], therefore the coalescence might not be affected to the same extent as when increasing the pH and promoting the dissociation of much more surface-active acidic species. Interestingly, even though some oils had a nondetectable TAN value, their coalescence at high pH was either extremely low (P5) or it was not possible perform measurements due to too low interfacial tension and instability of droplets (J, K). This probably means that the TAN value does not represent well the acidic components of crude oil, at least in relation to separation issues, as it gives no information on the structure of the acids [41]. However, after adding calcium to the high pH brine, the coalescence almost always improved. This was most likely caused by the complexation of some acidic species present at the interface by calcium. Subsequently, these complexes became less surface-active or even diffused to the oil phase [42].

The addition of the dissolved components to the water phase prompted an oil-specific response. In some cases the coalescence stayed at the same level or even slightly increased, but the majority of oils experienced decreased coalescence. There is no clear indication from the properties or chemical composition of the oils on why some oils behaved in a specific manner. All of the oils with increased coalescence frequency upon the addition of dissolved acids (B, H, P3) had TAN below detection limit, however the rest of the crude oils with

similar TAN (I, K and P5) did not have the same trend. Furthermore, we previously argued that the increase or decrease of coalescence could be the result of the direction of the mass transfer to or from the dispersed phase [31], which was found to affect coalescence in a certain way [43, 44]. Unfortunately, the experiments presented here did not show any additional proof for that hypothesis. When the synthetic produced water was used, almost all the oils experienced a decrease or no change in coalescence (except crude oil H). This was most likely due to precipitation of carbonate salts and the adsorption of these precipitated particles at the oil-water interface, which would negatively impact the coalescence through Pickering stabilisation [45]. Specific interactions between the ions present in water and the surface-active components could offer another explanation for these results [24]. Finally, higher water viscosity (due to higher total dissolved solids content) could also contribute to the decrease of coalescence. The pH of the synthetic produced water was also higher (pH 7) than that of the standard sodium chloride brine. While additional measurements with sodium chloride brine at pH 7, performed for selected oils, showed a small decrease of coalescence, this effect was not as significant as for the synthetic produced water.

In an attempt to find correlations between the physicochemical properties of the crude oils and the coalescence in all systems, multivariate analysis was performed. The results of the PLS analysis for coalescence in pH 4 and pH 6 conditions are shown in Figure 6. Similar plots for coalescence in pH 10 brines can be seen in Figure S2 in SI.

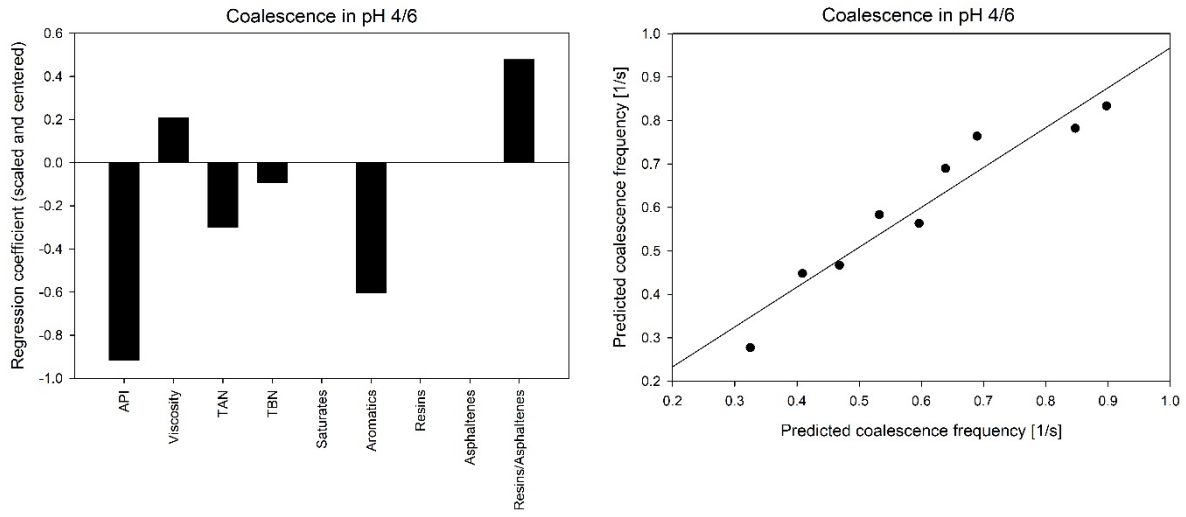

Figure 6 Regression coefficients for factors contributing to coalescence frequency (left) and predicted vs measured plot based on the PLS regression model (right).

It should be noted that crude oil H was excluded from the analysis in both conditions due to its unique behaviour in almost all the systems. In the case of pH 4/6 results, the variable importance in projection analysis suggested including only six out of nine X-variables in the final PLS regression model: API° gravity, viscosity, TAN, TBN, aromatics content and resin-to-asphaltene ratio. With these values, the model was re-calculated and the results are shown in Figure 6. Positive regression coefficients signify the direct correlation between the factor and the response, while negative suggest inverse relationship. It can be observed that the lighter the oil (higher API, lower viscosity), the lower the coalescence frequency is predicted to be. Also, higher content of acidic and basic species, often surface-active, could also contribute to reduced coalescence. Similarly, the increased aromatics content in crude oil was another factor causing the decrease of coalescence. Interestingly, the increasing resin-to-asphaltenes ratio was found to positively affect coalescence. Resins are known to solvate and stabilize asphaltenes [46], which can lead to less stable emulsions. The resin to asphaltene ratio was found to be inversely proportional to the emulsion stability [47, 48] and also had an effect on the oil droplet film rigidity [49], which supports the findings observed here. With the calculated coefficients values, a well-fitted prediction model was plotted (R^2 = 0.92). The PLS analysis

of coalescence in pH 10 conditions was performed including all factors (all VIP values above 0.8), and in general shows similar trends. It should be noted, however, that a significant (negative) correlation was observed for the resins content. Since the interfacially-active naphthenic acids are often included in that crude oil SARA fraction [50], higher pH conditions could have increased the importance of these components due to their dissociation and adsorption at the oil-water interface. The model had a slightly worse fit (R^2 = 0.81) compared to the lower pH conditions, but still predicted the coalescence frequency relatively well.

3.2. Coalescence time of crude oil droplets

Coalescence time measurements were performed on selected systems. The results are shown as lognormal distributions, rather than average values, due to the large spread of data (Figure 7a-c).

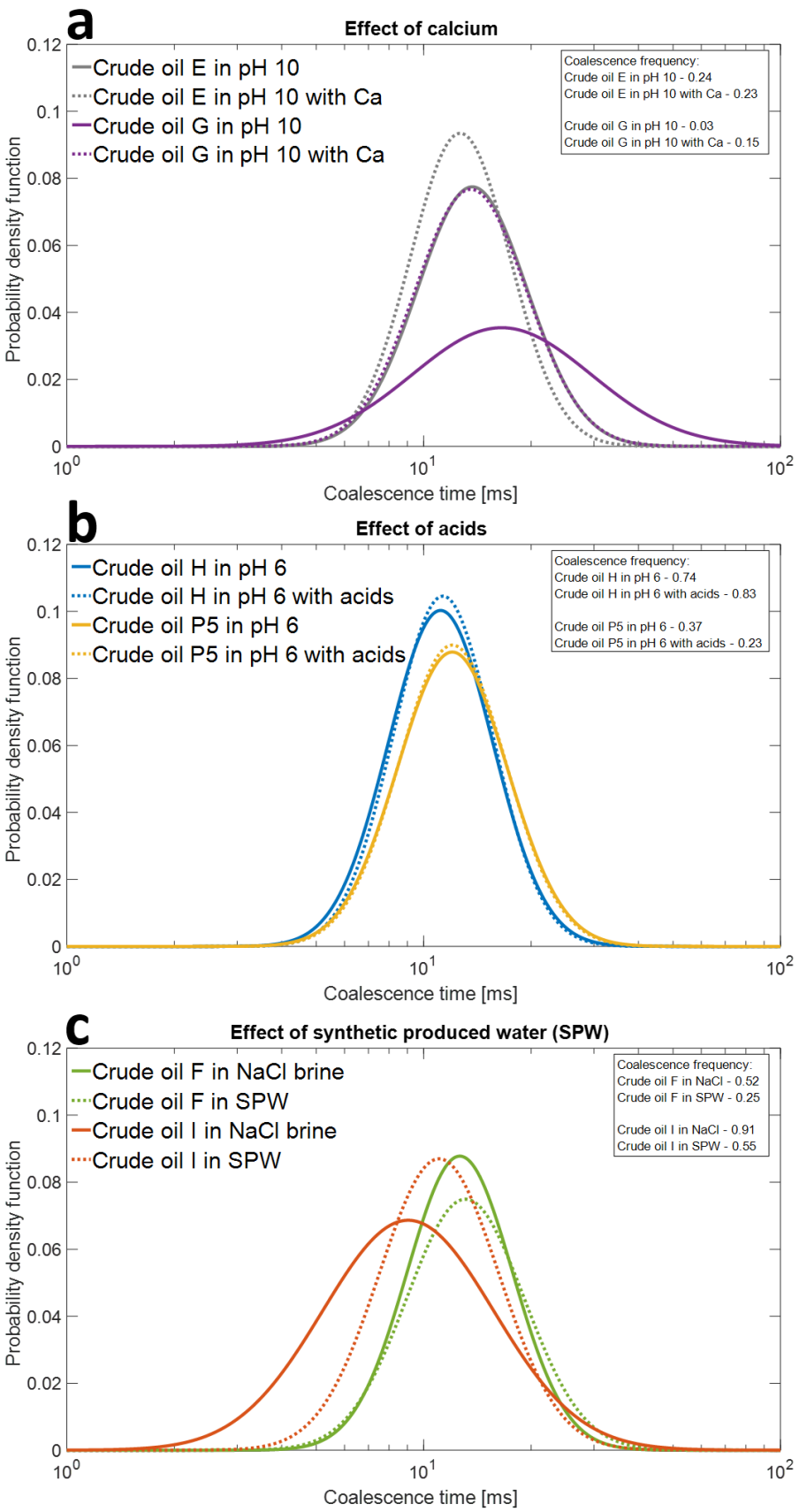

Figure 7 Coalescence time distributions of crude oils in different conditions.

Each distribution was plotted based on at least 2000 individual coalescence events. Furthermore, only the coalescence times of merging between two initial-sized droplets were included in the distributions. Some systems coalesced more readily than others (see values of the coalescence frequencies in the insets in Figure 7), which meant that the contribution from the coalescence times between larger droplets would have been more significant. As shown previously [37] and below, the size of the coalescing droplets has a substantial effect on the coalescence time.

Coalescence of crude oils E and G in sodium chloride brine at pH 10 was slower than in the brine containing calcium, and a larger difference was observed for crude oil G, both in the width of the distribution and its mode. It was also noted that crude oil E had lower coalescence times, compared to oil G. In contrast, the addition of acids had hardly any effect on the coalescence times of both studied oils. Still, crude oil H coalesced faster than the other oil. When the coalescence times of crude oils F and I in sodium chloride brine at pH 6 and synthetic produced water were compared, the coalescence took longer for the latter water phase (larger difference was observed for crude oil I).

The effect of calcium on the drainage time is consistent with the previously outlined explanation for the improved coalescence upon addition of the divalent ions at higher pH. Calcium has the ability to bind some of the acidic species at the interface, which can either lead to their diffusion to the bulk oil phase or reduced interfacial activity. This could decrease the Marangoni flux, which counteracts the film drainage. When comparing coalescence times to the corresponding coalescence frequencies in the same systems, the results are consistent in the case of crude oil G, where a large decrease in coalescence times could have been the reason for the five-fold increase of coalescence frequency. Crude oil E had no difference in coalescence frequencies between calcium/no calcium systems, and the difference in coalescence times was also very small. For studying the effect of acids, two systems with

opposite response were chosen for the coalescence time studies. In both cases the coalescence time distributions with and without acids were overlapping, showing no significant influence of these components on the drainage times. Unfortunately, we could not find an explanation for this result. Still, crude oil H had lower coalescence times than oil P5, which was also reflected in the higher coalescence frequencies values. While the presence of divalent cations in the synthetic produced water should have had a positive effect on the coalescence time, as shown above and elsewhere [24], it is clear that the more complex ionic composition and even the possible presence of some precipitated salts, lead to longer coalescence times. This could have been caused by the slightly higher pH of the brine and therefore higher interfacial activity of the acidic species in the crude oils.

The effect of the droplet size on the coalescence time of crude oil H in NaCl brine at pH 6 was shown in Figure 8. Here drops were divided into size classes, where size class 1 represents the initial size of droplets, size class 2 refers to a droplet formed out of two size class 1 drops and so on. Each line in Figure 8 represents coalescence events between specific size classes, i.e. 1:1 refers to coalescence between two size class 1 drops, 1:2 between droplets of size class 1 and 2 etc. In this case, the coalescence time distributions were plotted based on a lower amount of merging events due to the limited coalescence between droplets of larger sizes. Still, at least 150 events were captured for all distributions (except of the 3:3 result, where only 20 data points were obtained).

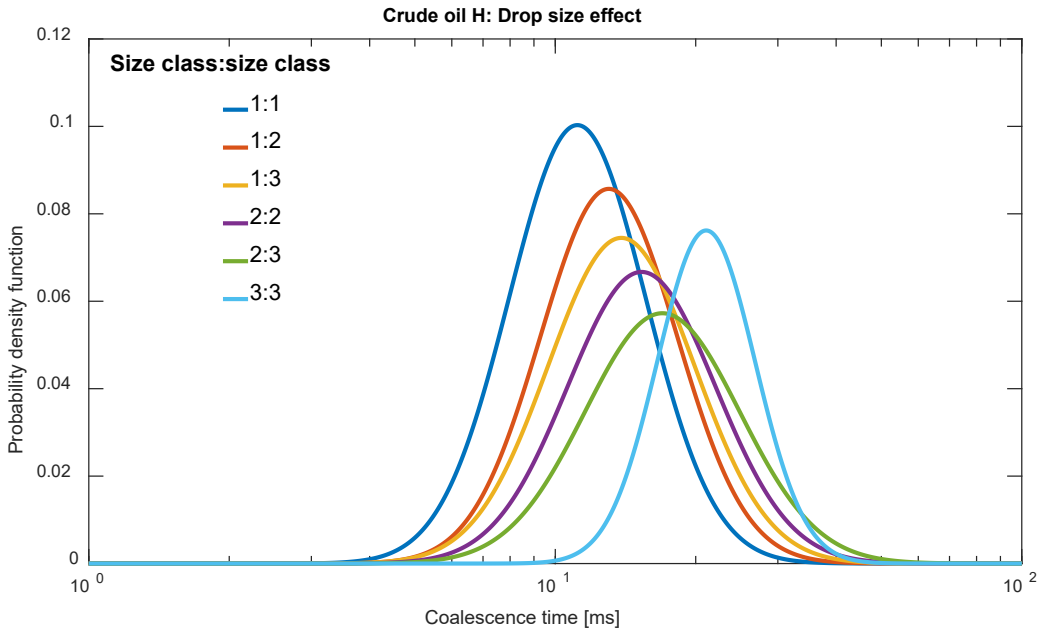

Figure 8 Coalescence time distributions of crude oil H droplets of various sizes in sodium chloride brine at pH 6.

It is clear that the coalescence time was shorter for the smaller droplets. The modes of coalescence time distributions of merging between 1:1, 2:2 and 3:3 size classes increased from 11 ms to 15 ms and to 21 ms, for the respective cases. It is also worth mentioning that when a droplet of class size 4 could have been formed in two possible ways (1:3 or 2:2), the coalescence was shorter for a system with a smaller droplet involved in the event.

The results obtained here are in line with our previous findings for model oils [37] and agree with coalescence models [6, 51]. The droplet size is the most important parameter affecting the duration of coalescence. With increase of the droplet size, the volume of liquid needed to be drained also increases, which prolongs the drainage process. Interestingly, while the coalescence of 1:1 size classes was quite similar to the coalescence of the same droplets made of dodecane (11 ms and 10.5 ms, respectively), the difference between the model oil and crude oil increased drastically with the droplet size (for the 3:3 case, the modes of coalescence time were equal to 21 ms and 13.5 ms for the crude oil and model oil,

respectively). This was most likely caused by the presence of surface-active components with different molecular structure in the crude oil.

3.3. Droplet ageing effect

The effect of droplet ageing was studied in two ways. In the first approach, the coalescence channel dimensions were the same as in the first section, whereas the length of the meandering channel after T-junction, but before entering the coalescence chamber, was changed (designs were inspired by the work of Muiljwijk et al. [52]). The resulting droplet ageing time before the possibility of coalescence was, from the shortest to the longest channels, ca. 5, 25 and 125 ms. Varying the ageing channel length did not affect the droplet size nor their number. In the second approach, a chip with a significantly longer and slightly wider coalescence channel was used. The resulting residence time inside the chip was more than seven times longer than for the other chips used to study coalescence frequency. It also allowed to study more closely the evolution of the size distribution in five different parts of the microfluidic chip during the flow of droplets.

The results obtained with the first approach were presented in Figure 9.

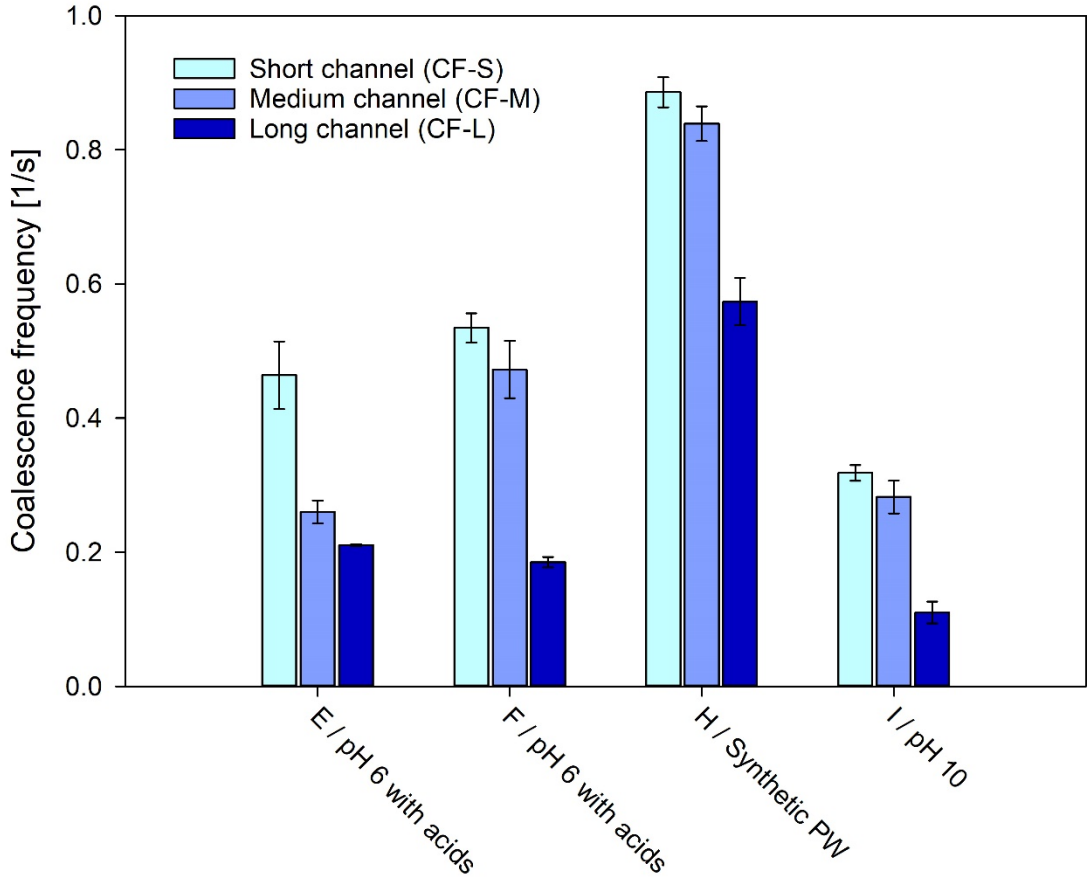

Figure 9 Coalescence frequencies of crude oil droplets in various conditions as a function of their ageing time.

The highest coalescence frequencies were always measured for the shortest equilibration time (using chip CF-S), regardless of the oil or water phase, while the least coalescence was observed for the longest meandering channel (CF-L). The relative coalescence frequency difference between the various ageing times, however, was found to be system-dependent. In the case of crude oil E in pH 6 brine with dissolved components, the largest decrease of coalescence occurred between the CF-S and CF-M chips. In other systems, the coalescence decline was the most prominent between the medium and long channels.

Upon creation of a new interface (i.e. drop formation from the bulk oil phase), interfacially active components start to diffuse to the oil-water interface, which decreases the interfacial

tension [11, 42] and leads to the formation of viscoelastic interfacial layers [53, 54] that affect their stability and likelihood of coalescence. In practice, ageing of an interface was shown to influence the coalescence frequency or time in various systems. Moran and Sumner studied merging of bitumen droplets in water with a micropipette technique and found that ageing droplets can greatly decrease the coalescence probability [55], which is in line with the results obtained here. With their drop coalescence and rheology experiments, Harbottle et al. were able to link the shear rheological properties of the aged oil-water interface with the coalescence time between two water drops [56]. The increasingly higher elastic response, originating from the adsorption and rearrangement of asphaltenes at the interface, was found to be the main reason behind the stability of the aged systems. Nowbahar et al., who investigated the coalescence of water droplets in diluted bitumen with a microfluidic device, also found that ageing the emulsion leads to reduced or no coalescence [32]. Other authors had similar observations [22, 52].

The relative difference between coalescence frequencies, measured with chips with different aging channel lengths, can also point to the adsorption kinetics of oil components diffusing to the interface. By taking into consideration only the uninterrupted diffusion of components to the oil-water interface, the longest meandering channel probably provided sufficient residence time for the 50-60 μm droplet generated in the present microfluidic device to reach a quasi-equilibrated state, at least in the orders of magnitude. This is in stark contrast with other techniques, where the larger size of droplets requires significantly longer ageing time (minutes or hours). Comparing crude oil E with other crude oils tested with these chip designs shows that it probably had lower molecular weight components that could diffuse faster, as indicated by the relative difference of coalescence frequencies between short and medium, and medium and long channel lengths. In the case of other oils, the significantly decreased coalescence frequencies, obtained with the CF-L chip, could indicate the

adsorption of asphaltenes and increased elasticity of the interface, leading to longer coalescence times. This type of information gives additional insight into the chemistry of crude oil and its effect on the emulsion stability. Furthermore, it can also be useful for determining the effect of production chemicals, designed to improve separation, on fresh or aged interfaces, as also shown by Nowbahar et al. [32].

The results from the second approach, showing the coalescence of four crude oils in pH 10 brine with calcium ions, are presented in Figure 10.

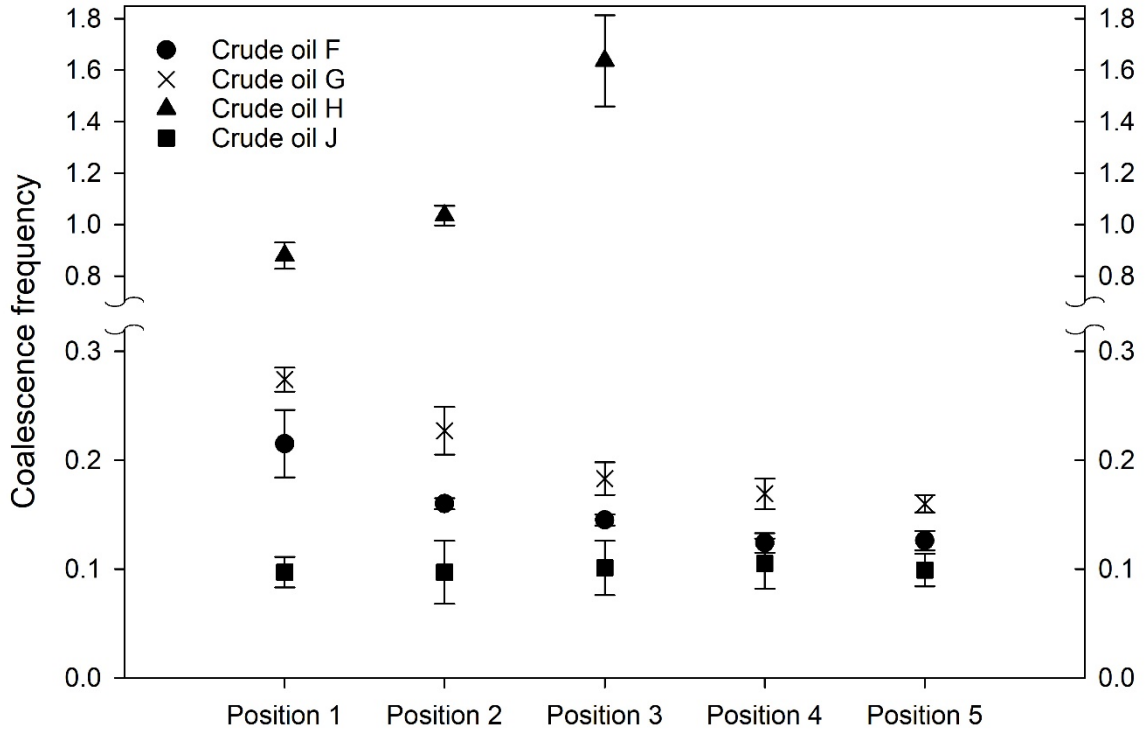

Figure 10 Coalescence frequencies of crude oils in sodium chloride brine with calcium at pH 10 as a function of the position in the coalescence channel.

Crude oils F and G behaved quite similarly. At the first position, the coalescence is the highest, after which it starts to gradually drop and seems to reach a plateau in the last two positions. In contrast, crude oil H was coalescing quite extensively, and the coalescence frequency increased at the positions 2 and 3. Due to the size of the droplets (>400 µm) and

their tendency to deform, it was not possible to perform image analysis past this recording point. The coalescence frequency of crude oil J was constant throughout all recording points. It should also be pointed out that due to different dimensions of the channels, the velocity and droplet distribution in the channel changed, which in most cases reduced the coalescence frequency as compared to the values shown in Figure 4. Only in the case of crude oil J, the coalescence was similar or even slightly higher. However, the trends in merging remained the same – crude oil H had the highest coalescence, followed by G, F and J, respectively.

The coalescence frequency should probably be expected to decrease with the residence time in the channel, as noted for crude oils F and G. Not only the droplets have more time to age in the surrounding water phase, but also the coalescence time of bigger droplets is higher, as seen from Figure 8, which typically leads to reduced coalescence frequency. The information on the number of droplets of each size could be used for generating size distributions and that is presented in Figure 11, where the volumetric size distributions of crude oil G and H droplets were plotted as a function of the position in the coalescence channel.

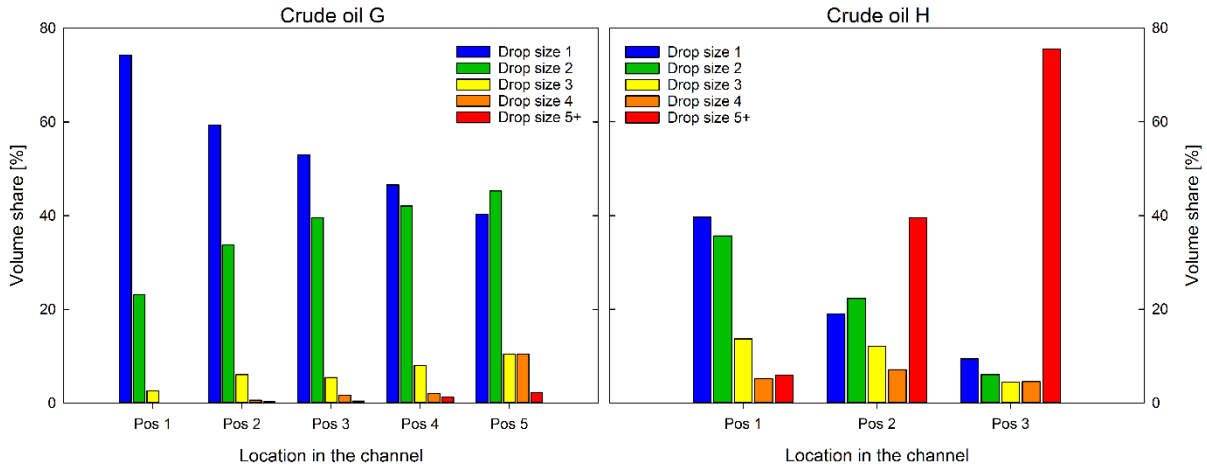

Figure 11 Volumetric size distributions of crude oil G and H droplets of different sizes as a function of position in the coalescence channel.

The droplets were divided into size classes, similar to the coalescence time analysis. As a result of high coalescence frequency for crude oil G in the beginning of the channel, the

initial decrease of the share of size class 1 droplets was high, however the absolute difference was also lower between the consecutive sections. This means that the number of initial size droplets and collisions between them had the largest effect on the high coalescence frequency at the first section for this oil. After that, the total amount of droplets decreases, which reduced the chances for collision between droplets and possible coalescence, thereby decreasing the coalescence frequency. Similar observation was made for crude oil F.

Interestingly, crude oil J did not behave in the same way. This could probably be explained by its low coalescence frequency. The total number of droplets did not decrease as drastically as for the other two crude oils. For crude oil J, it decreased by ca. 5% between each recording point, while the other oils had a larger than 10% decline in the first two sections of the channel. This means that the total number of crude oil J droplets in the channel at the outlet was approximately the same as that value for oils F and G, but at the first or second point. Similar can be said about the number of initial-sized droplets, where the volumetric share of 60% for crude oil J at the last recording point, have already been obtained at sections 2 and 3 for crude oil G and F, respectively.

Lastly, crude oil H again behaved uniquely, as in the other experiments. The coalescence frequency was very high to begin with and already at the first recording point the reduction in the total number of droplets reached 40%. Figure 11 also shows that the share of crude oil H droplets of initial size was almost equal to the volume contributions of the class two droplets. Already at the second position, the volumetric share of drop sizes equal or larger than 5 was dominant and increased dramatically in the next position. The overall large size of droplets could probably explain why the coalescence frequency for this oil continued to increase for all recording positions. Since the coalescence experiments are measured in a relatively narrow channel, the droplets have limited space to move. In most cases, the diameter of a single droplet is ca. 10% of the width of the channel. In the case of crude oil H, where the

droplets after second recording point would often be larger than 250-300 μm, the drop diameter to channel width ratio increased significantly. With these space limitations, many droplets were forced into contact, which eventually led to coalescence between them and formation of even larger drops. At the end of the coalescence chamber, the droplets of crude oil H in these conditions would often be larger than the width of the channel and prone to deformation or even, in some cases, breakage.

4. Conclusions

In this paper, we have presented a study of the crude oil droplet coalescence in produced water. A number of different crude oils and water phases were used to reveal some correlations between the chemical composition of both phases and the extent of merging. We have shown that the coalescence is typically highest in the lower or neutral pH and with less complex water composition, however this was crude oil-dependent. The coalescence frequency results corresponded well with the supplementary coalescence time measurements, which could often explain the change in coalescence behaviour. Furthermore, the experiments indicated that the droplets merged more readily right after formation, whereas coalescence was impeded when they were allowed to age. In addition, it was found that larger droplets coalesced slower, which could have led to a reduction of the coalescence frequency in the long channel experiments. The methodologies and results presented in this paper emphasize the importance of the chemical properties on the coalescence process, which will also have significant implications for the water quality during and after the produced water treatment processes.

ACKNOWLEDGMENTS

This work was carried out as a part of SUBPRO, a Research-based Innovation Centre within Subsea Production and Processing. The authors gratefully acknowledge the financial support

from SUBPRO, which is financed by the Research Council of Norway, major industry partners and NTNU. We additionally thank AkerBP, Equinor, Lundin, Neptune Energy and Shell for oil samples, and Diana Fernandes for performing crude oil analyses.

REFERENCES

1. Weschenfelder, S. E.; Louvisse, A. M. T.; Borges, C. P.; Meabe, E.; Izquierdo, J.; Campos, J. C., Evaluation of ceramic membranes for oilfield produced water treatment aiming reinjection in offshore units. *Journal of Petroleum Science and Engineering* **2015,** *131*, 51-57.
2. Arnold, K.; Stewart, M.; Stewart, M. I.; Stewart, M. I., *Surface Production Operations: Design of Oil-Handling Systems and Facilities*. Second ed.; Gulf Professional Publishing: Woburn, 1999.
3. Saththasivam, J.; Loganathan, K.; Sarp, S., An overview of oil–water separation using gas flotation systems. *Chemosphere* **2016,** *144*, 671-680.
4. Dudek, M.; Øye, G., Microfluidic Study on the Attachment of Crude Oil Droplets to Gas Bubbles. *Energy Fuels* **2018,** *32* (10), 10513-10521.
5. Dickhout, J. M.; Moreno, J.; Biesheuvel, P. M.; Boels, L.; Lammertink, R. G. H.; de Vos, W. M., Produced water treatment by membranes: A review from a colloidal perspective. *J. Colloid Interface Sci.* **2017,** *487*, 523-534.
6. Chesters, A. K., The modelling of coalescence processes in fluid-liquid dispersions: a review of current understanding. *Chem. Eng. Res. Des.* **1991,** *69* (A4), 259-270.
7. Gaweł, B.; Lesaint, C.; Bandyopadhyay, S.; Øye, G., Role of Physicochemical and Interfacial Properties on the Binary Coalescence of Crude Oil Drops in Synthetic Produced Water. *Energy Fuels* **2015,** *29* (2), 512-519.
8. Arla, D.; Sinquin, A.; Palermo, T.; Hurtevent, C.; Graciaa, A.; Dicharry, C., Influence of pH and Water Content on the Type and Stability of Acidic Crude Oil Emulsions. *Energy Fuels* **2007,** *21* (3), 1337-1342.
9. Dudek, M.; Kancir, E.; Øye, G., Influence of the Crude Oil and Water Compositions on the Quality of Synthetic Produced Water. *Energy Fuels* **2017,** *31* (4), 3708-3716.
10. Angle, C. W.; Hamza, H. A.; Dabros, T., Size distributions and stability of toluene diluted heavy oil emulsions. *AlChE J.* **2006,** *52* (3), 1257-1266.
11. Poteau, S.; Argillier, J.-F.; Langevin, D.; Pincet, F.; Perez, E., Influence of pH on Stability and Dynamic Properties of Asphaltenes and Other Amphiphilic Molecules at the Oil−Water Interface†. *Energy Fuels* **2005,** *19* (4), 1337-1341.
12. Krawczyk, M. A.; Wasan, D. T.; Shetty, C., Chemical demulsification of petroleum emulsions using oil-soluble demulsifiers. *Industrial & Engineering Chemistry Research* **1991,** *30* (2), 367-375.
13. Mohammed, R. A.; Bailey, A. I.; Luckham, P. F.; Taylor, S. E., Dewatering of crude oil emulsions 3. Emulsion resolution by chemical means. *Colloids Surf. Physicochem. Eng. Aspects* **1994,** *83* (3), 261-271.
14. Peña, A. A.; Hirasaki, G. J.; Miller, C. A., Chemically Induced Destabilization of Water-in-Crude Oil Emulsions. *Industrial & Engineering Chemistry Research* **2005,** *44* (5), 1139-1149.
15. Mhatre, S.; Simon, S.; Sjöblom, J.; Xu, Z., Demulsifier assisted film thinning and coalescence in crude oil emulsions under DC electric fields. *Chem. Eng. Res. Des.* **2018,** *134*, 117-129.
16. Kang, W.; Yin, X.; Yang, H.; Zhao, Y.; Huang, Z.; Hou, X.; Sarsenbekuly, B.; Zhu, Z.; Wang, P.; Zhang, X.; Geng, J.; Aidarova, S., Demulsification performance, behavior and mechanism of

different demulsifiers on the light crude oil emulsions. *Colloids Surf. Physicochem. Eng. Aspects* **2018,** *545*, 197-204.
17. Hjartnes, T. N.; Sørland, G. H.; Simon, S.; Sjöblom, J., Demulsification of Crude Oil Emulsions Tracked by Pulsed Field Gradient (PFG) Nuclear Magnetic Resonance (NMR). Part I: Chemical Demulsification. *Industrial & Engineering Chemistry Research* **2019,** *58* (6), 2310-2323.
18. Kim, Y. H.; Wasan, D. T.; Breen, P. J., A study of dynamic interfacial mechanisms for demulsification of water-in-oil emulsions. *Colloids Surf. Physicochem. Eng. Aspects* **1995,** *95* (2), 235-247.
19. Bhardwaj, A.; Hartland, S., Kinetics of coalescence of water droplets in water-in-crude-oil emulsions. *J. Dispersion Sci. Technol.* **1994,** *15* (2), 133-146.
20. Chen, T. Y.; Mohammed, R. A.; Bailey, A. I.; Luckham, P. F.; Taylor, S. E., Dewatering of crude oil emulsions 4. Emulsion resolution by the application of an electric field. *Colloids Surf. Physicochem. Eng. Aspects* **1994,** *83* (3), 273-284.
21. Peru, D. A.; Lorenz, P. B., The Effect of Equilibration Time and Temperature on Drop-Drop Coalescence of Wilmington Crude Oil in a Weakly Alkaline Brine. *Chem. Eng. Commun.* **1989,** *77* (1), 91-114.
22. Ata, S.; Pugh, R. J.; Jameson, G. J., The influence of interfacial ageing and temperature on the coalescence of oil droplets in water. *Colloids Surf. Physicochem. Eng. Aspects* **2011,** *374* (1–3), 96-101.
23. Ayirala, S. C.; Al-Saleh, S. H.; Al-Yousef, A. A., Microscopic scale interactions of water ions at crude oil/water interface and their impact on oil mobilization in advanced water flooding. *Journal of Petroleum Science and Engineering* **2018,** *163*, 640-649.
24. Ayirala, S. C.; Yousef, A. A.; Li, Z.; Xu, Z., Coalescence of Crude Oil Droplets in Brine Systems: Effect of Individual Electrolytes. *Energy Fuels* **2018,** *32* (5), 5763-5771.
25. Sterling Jr, M. C.; Ojo, T.; Autenrieth, R. L.; Bonner, J. S.; Page, C. A.; Ernest, A. N. S. In *Coalescence kinetics of dispersed crude oil in a laboratory reactor*, Environment Canada Arctic and Marine Oil Spill Program Technical Seminar (AMOP) Proceedings, 2002; pp 741-753.
26. Angle, C. W.; Hamza, H. A., Drop sizes during turbulent mixing of toluene–heavy oil fractions in water. *AlChE J.* **2006,** *52* (7), 2639-2650.
27. Angle, C. W.; Hamza, H. A., Effects of sand and process water pH on toluene diluted heavy oil in water emulsions in turbulent flow. *AlChE J.* **2009,** *55* (1), 232-242.
28. Silset, A.; Flåten, G. R.; Helness, H.; Melin, E.; Øye, G.; Sjöblom, J., A Multivariate Analysis on the Influence of Indigenous Crude Oil Components on the Quality of Produced Water. Comparison Between Bench and Rig Scale Experiments. *J. Dispersion Sci. Technol.* **2010,** *31* (3), 392-408.
29. Eftekhardadkhah, M.; Øye, G., Correlations between crude oil composition and produced water quality: A multivariate analysis approach. *Ind. Eng. Chem. Res.* **2013,** *52* (48), 17315-17321.
30. Bremond, N.; Bibette, J., Exploring emulsion science with microfluidics. *Soft Matter* **2012,** *8* (41), 10549-10559.
31. Dudek, M.; Bertheussen, A.; Dumaire, T.; Øye, G., Microfluidic Tools for Studying Coalescence of Crude Oil Droplets in Produced Water. *Chem. Eng. Sci.* **2018,** *191*, 448-458.
32. Nowbahar, A.; Whitaker, K. A.; Schmitt, A. K.; Kuo, T.-C., Mechanistic Study of Water Droplet Coalescence and Flocculation in Diluted Bitumen Emulsions with Additives Using Microfluidics. *Energy Fuels* **2017,** *31* (10), 10555-10565.
33. Lin, Y.-J.; Perrard, A.; Biswal, S. L.; Hill, R. M.; Trabelsi, S., Microfluidic Investigation of Asphaltenes-Stabilized Water-in-Oil Emulsions. *Energy Fuels* **2018**.
34. Loufakis, D. N.; Schmitt, A. K.; Nelson, C.; Hoyles, S.; Goodwin, J.; White, B.; Ayers, C., A Microfludic Technique for the Evaluation of Demulsifiers. In *SPE International Conference on Oilfield Chemistry*, Society of Petroleum Engineers: Montgomery, Texas, USA, 2017; p 9.

35. Hannisdal, A.; Hemmingsen, P. V.; Sjöblom, J., Group-Type Analysis of Heavy Crude Oils Using Vibrational Spectroscopy in Combination with Multivariate Analysis. *Industrial & Engineering Chemistry Research* **2005,** *44* (5), 1349-1357.
36. Dudek, M.; Muijlwijk, K.; Schroen, C. G. P. H.; Øye, G., The effect of dissolved gas on coalescence of oil drops studied with microfluidics. *J. Colloid Interface Sci.* **2018,** *528*, 166-173.
37. Dudek, M.; Fernandes, D.; Helno Herø, E.; Øye, G., Microfluidic method for determining drop-drop coalescence and contact times in flow. *Colloids Surf. Physicochem. Eng. Aspects* **2019**, 124265.
38. Nenningsland, A. L.; Simon, S.; Sjöblom, J., Surface Properties of Basic Components Extracted from Petroleum Crude Oil. *Energy Fuels* **2010,** *24* (12), 6501-6505.
39. Eftekhardadkhah, M.; Kløcker, K. N.; Trapnes, H. H.; Gaweł, B.; Øye, G., Composition and Dynamic Adsorption of Crude Oil Components Dissolved in Synthetic Produced Water at Different pH Values. *Ind. Eng. Chem. Res.* **2016,** *55* (11), 3084-3090.
40. Bertheussen, A.; Simon, S.; Sjöblom, J., Equilibrium partitioning of naphthenic acids and bases and their consequences on interfacial properties. *Colloids Surf. Physicochem. Eng. Aspects* **2017,** *529* (Supplement C), 45-56.
41. Jones, D. M.; Watson, J. S.; Meredith, W.; Chen, M.; Bennett, B., Determination of Naphthenic Acids in Crude Oils Using Nonaqueous Ion Exchange Solid-Phase Extraction. *Anal. Chem.* **2001,** *73* (3), 703-707.
42. Tichelkamp, T.; Teigen, E.; Nourani, M.; Øye, G., Systematic study of the effect of electrolyte composition on interfacial tensions between surfactant solutions and crude oils. *Chem. Eng. Sci.* **2015,** *132*, 244-249.
43. Groothuis, H.; Zuiderweg, F. J., Influence of mass transfer on coalescence of drops. *Chem. Eng. Sci.* **1960,** *12* (4), 288-289.
44. Chevaillier, J. P.; Klaseboer, E.; Masbernat, O.; Gourdon, C., Effect of mass transfer on the film drainage between colliding drops. *J. Colloid Interface Sci.* **2006,** *299* (1), 472-485.
45. Binks, B. P.; Rodrigues, J. A.; Frith, W. J., Synergistic Interaction in Emulsions Stabilized by a Mixture of Silica Nanoparticles and Cationic Surfactant. *Langmuir* **2007,** *23* (7), 3626-3636.
46. Murgich, J.; Strausz, O. P., Molecular Mechanics of Aggregates of Asphaltenes and Resins of the Athabasca Oil. *Pet. Sci. Technol.* **2001,** *19* (1-2), 231-243.
47. Spiecker, P. M.; Gawrys, K. L.; Trail, C. B.; Kilpatrick, P. K., Effects of petroleum resins on asphaltene aggregation and water-in-oil emulsion formation. *Colloids Surf. Physicochem. Eng. Aspects* **2003,** *220* (1), 9-27.
48. Schorling, P. C.; Kessel, D. G.; Rahimian, I., Influence of the crude oil resin/asphaltene ratio on the stability of oil/water emulsions. *Colloids Surf. Physicochem. Eng. Aspects* **1999,** *152* (1), 95-102.
49. Strassner, J. E., Effect of pH on Interfacial Films and Stability of Crude Oil-Water Emulsions. **1968**.
50. Carbonezi, C. A.; de Almeida, L. C.; Araujo, B. C.; Lucas, E. F.; González, G., Solution Behavior of Naphthenic Acids and Its Effect on the Asphaltenes Precipitation Onset. *Energy Fuels* **2009,** *23* (3), 1249-1252.
51. Liao, Y.; Lucas, D., A literature review on mechanisms and models for the coalescence process of fluid particles. *Chem. Eng. Sci.* **2010,** *65* (10), 2851-2864.
52. Muijlwijk, K.; Colijn, I.; Harsono, H.; Krebs, T.; Berton-Carabin, C.; Schroën, K., Coalescence of protein-stabilised emulsions studied with microfluidics. *Food Hydrocolloids* **2017,** *70*, 96-104.
53. Spiecker, P. M.; Kilpatrick, P. K., Interfacial Rheology of Petroleum Asphaltenes at the Oil−Water Interface. *Langmuir* **2004,** *20* (10), 4022-4032.
54. Arla, D.; Flesisnki, L.; Bouriat, P.; Dicharry, C., Influence of Alkaline pH on the Rheology of Water/Acidic Crude Oil Interface. *Energy Fuels* **2011,** *25* (3), 1118-1126.
55. Moran, K.; Sumner, R. J., Aging Effects on Surface Properties and Coalescence of Bitumen Droplets. *The Canadian Journal of Chemical Engineering* **2007,** *85* (5), 643-653.

56. Harbottle, D.; Chen, Q.; Moorthy, K.; Wang, L.; Xu, S.; Liu, Q.; Sjoblom, J.; Xu, Z., Problematic Stabilizing Films in Petroleum Emulsions: Shear Rheological Response of Viscoelastic Asphaltene Films and the Effect on Drop Coalescence. *Langmuir* **2014,** *30* (23), 6730-6738.